Intermittent collective dynamics emerge from conflicting imperatives in sheep herds

Francesco Ginelli[a,1,2], Fernando Peruani[b,2], Marie-Helène Pillot[c,d], Hugues Chaté[e,f], Guy Theraulaz[c,d], and Richard Bon[c,d]

[a]Physics Department and Institute for Complex Systems and Mathematical Biology, King's College, University of Aberdeen, Aberdeen AB24 3UE, United Kingdom; [b]Laboratoire J.A. Dieudonné, Université de Nice Sophia Antipolis, UMR CNRS 6621, 06108 Nice Cedex 02, France; [c]Centre de Recherches sur la Cognition Animale, UMR-CNRS 5169, Universit Paul Sabatier, 31062 Toulouse Cedex 9, France; [d]CNRS, Centre de Recherches sur la Cognition Animale, F-31062 Toulouse, France; [e]Service de Physique de l'État Condensé, CNRS UMR 3680, Commissariat à l'énergie atomique et aux énergies alternatives (CEA)–Saclay, 91191 Gif-sur-Yvette, France; and [f]Beijing Computational Science Research Center, Beijing 100094, China

Edited by Giorgio Parisi, University of Rome, Rome, Italy, and approved August 18, 2015 (received for review February 25, 2015)

Among the many fascinating examples of collective behavior exhibited by animal groups, some species are known to alternate slow group dispersion in space with rapid aggregation phenomena induced by a sudden behavioral shift at the individual level. We study this phenomenon quantitatively in large groups of grazing Merino sheep under controlled experimental conditions. Our analysis reveals strongly intermittent collective dynamics consisting of fast, avalanche-like regrouping events distributed on all experimentally accessible scales. As a proof of principle, we introduce an agent-based model with individual behavioral shifts, which we show to account faithfully for all collective properties observed. This offers, in turn, an insight on the individual stimulus/response functions that can generate such intermittent behavior. In particular, the intensity of sheep allelomimetic behavior plays a key role in the group's ability to increase the per capita grazing surface while minimizing the time needed to regroup into a tightly packed configuration. We conclude that the emergent behavior reported probably arises from the necessity to balance two conflicting imperatives: (*i*) the exploration of foraging space by individuals and (*ii*) the protection from predators offered by being part of large, cohesive groups. We discuss our results in the context of the current debate about criticality in biology.

sheep herds | collective behavior | self-organization | computational modeling | Allelomimetism

The social interactions and behavioral mechanisms involved in the coordination of collective movements in animal groups largely determine the animals' ability to display adapted responses when they face challenges, such as finding, efficiently, food sources (1–4) or safe resting places (5–7) or avoiding predators (8–13). Thus, the diversity of collective motion patterns observed in group-living species reflects the multiple forms of interactions individuals use for coordinating their behavioral actions (14, 15). Deciphering these interactions, their relation with the patterns emerging at the collective level, and their connections with the physiological and ecological constraints peculiar to each group-living species is crucial to understanding the evolution of collective phenomena in biological systems (16–18). So far, only a handful of quantitative datasets have been gathered for large animal groups (19–21). Most of them have focused on elementary cases where the prevailing biological imperative seems to be group cohesion, either to gain protection from potential predators, such as for the spontaneous collective motion exhibited by starling flocks (19, 22) and some fish schools (23–25), or for reproductive purposes, as in swarms of midges (21, 26).

One important and, so far, often neglected aspect of collective motion is the existence of individual-level behavioral shifts, which, in turn, may trigger a transition at the collective level. For instance, in many species of fish, groups regularly alternate between a swarming state, in which fish simply aggregate with a low level of polarization, and a schooling state, in which individuals are aligned and move in the same direction (27, 28). This transition is elicited by a sudden change in the velocity of a single or a few individuals that propagates to the whole group. In many cases, the behavioral shift occurs without any perceived threat in the neighborhood, resulting in a spontaneous transition at the collective level that can be interpreted as a consequence of random individual decisions. Such alternating behavioral phases at the collective level have also been reported in refs. 29, 30.

Here, we report a quantitative study of the collective behavior of large groups of Merino sheep (*Ovis Aries*), a highly gregarious domestic breed (31), under controlled experimental conditions. Our analysis reveals an intermittent collective dynamics where long dispersion phases—during which grazing sheep slowly spread out, exploring the foraging field—are punctuated by fast packing events, triggered by an individual-level behavioral shift. We find that these events are distributed on all experimentally accessible scales. To gain insight on the sheep individual stimulus/response function, we introduce an agent-based model that explicitly includes behavioral shifts and strong allelomimetic effects. Our model results suggest that the observed collective behavior can be generated when parameters quantifying allelomimetic behavior are sufficiently large. In this parameter range, sheep regrouping time is minimized, and a large per capita grazing surface is at sheep disposal during dispersion phases.

Experimental Results

We first observed the activities of large groups ($n = 100$) of same-age female sheep in an enclosed, flat, and spatially homogeneous square arena of 80×80 m. Five different 1-h-long trials were realized, during which sheep movements were recorded

Significance

We report and analyze quantitative field observations of large groups of Merino sheep. While grazing, these sheep must balance two competing needs: (*i*) the maximization of individual foraging space and (*ii*) the protection from predators offered by a large dense group. We show that they resolve this conflict by alternating slow foraging phases—during which the group spreads out—with fast packing events triggered by an individual-level behavioral shift. This leads to an intermittent collective dynamics with large density oscillations triggered by packing events on all accessible scales: a quasi-critical state. All our findings are well accounted for by an explicit model with individual behavioral shifts and strong allelomimetic properties.

Author contributions: H.C., G.T., and R.B. designed research; F.G., F.P., M.-H.P., and R.B. performed research; F.G., F.P., and H.C. analyzed data; and F.G., F.P., H.C., and G.T. wrote the paper.

The authors declare no conflict of interest.

This article is a PNAS Direct Submission.

Freely available online through the PNAS open access option.

[1]To whom correspondence should be addressed. Email: francesco.ginelli@abdn.ac.uk.

[2]F.G. and F.P. contributed equally to this work.

This article contains supporting information online at www.pnas.org/lookup/suppl/doi:10.1073/pnas.1503749112/-/DCSupplemental.

by taking high-resolution pictures of the arena at a rate of one frame per second, from the top of a 7-m-high tower located outside one of the arena corners (details can be found in *Materials and Methods*, see Fig. S1). Quickly after their introduction in the arena, sheep started grazing and moving around. While grazing, the herd spreads apart in smaller groups, with an expanding leading front (see Movie S1). This slow dispersion dynamics was brought to an end by fast packing events. These events are typically triggered when an individual located at the group periphery starts running toward the center of the group, recruiting more and more sheep into a compact, fast-moving herd before finally stopping almost synchronously, leaving a rather dense herd that then resumed grazing. The whole scenario repeated itself with a varying proportion of sheep involved in the packing and running events, with a typical timescale of about 15 min between the largest ones. No discernible external stimulus that could have triggered the behavioral switch to running was observed. Note that no audible vocalization occurred before or during packing events that could have been used as an alarm signal.

Because only a few of such group-spanning events can be observed in 1-h-long sessions, we performed a longer experiment (3.5 h) with the same group size to quantify and analyze the phenomenon with more accuracy (see Movies S2*A* and S2*B*). During this period, sheep kept their grazing behavior punctuated by fast packing events. In images taken from the watchtower, many sheep are partially hidden by others, making automated tracking impossible. Therefore, the location $\mathbf{r}_i^t$ and heading $\mathbf{s}_i^t$ (with $|\mathbf{s}|=1$) of every sheep have been identified manually with a sampling rate of 1 min (except for a single packing event studied with a 1-s sampling rate; see below). To also measure instantaneous sheep velocities $\mathbf{v}_i^t=(\mathbf{r}_i^{t+\Delta t}-\mathbf{r}_i^t)/\Delta t$, we actually processed, at the same 1-min sampling rate, two consecutive images (separated by $\Delta t=1$ s, our data-taking time step). We estimate a maximum experimental error of around $\Delta r=0.2$ m on sheep position and $\Delta v=0.3$ m/s on sheep speed (for a complete discussion of tracking errors, see *Materials and Methods*).

Collective Motion Patterns. We have quantified the alternation of slow grazing expansion and fast packing runs. The most direct measurement is the group area $S(t)$ covered by the herd at time t. We define $S(t)$ as the surface of the convex hull defined by the sheep positions. (The convex hull of a set of points is the smallest convex polygon including all of the points. It gives a feasible approximation of the foraging area controlled by the group at any instant.) The time series of $S(t)$ shown in Fig. 1*A*, reveals the 12 major spread/packing events observed. Its autocorrelation time can be estimated to be around 5 min, being significantly larger than our chosen sampling time of 1 min, so that no significant information is lost due to our sampling choice.

The timescale of packing events can be characterized by the change of the group area over 1 min, $dS(t)\equiv S(t)-S(t-1)$. The time series is characterized by large negative spikes, indicating that the global contraction events take place on a much faster timescale than the slow spreading observed during grazing. Moreover, the parametric plot of $dS(t)$ vs. $S(t)$ for the major packing events shows that their dynamics, although being characterized by a rather strong stochastic component, tend to be all of the more abrupt as the maximum group area reached is larger (see Fig. 1*C*). The densest configuration observed covers about 75 m^2, whereas the most diluted state stretches over 2,329 m^2,

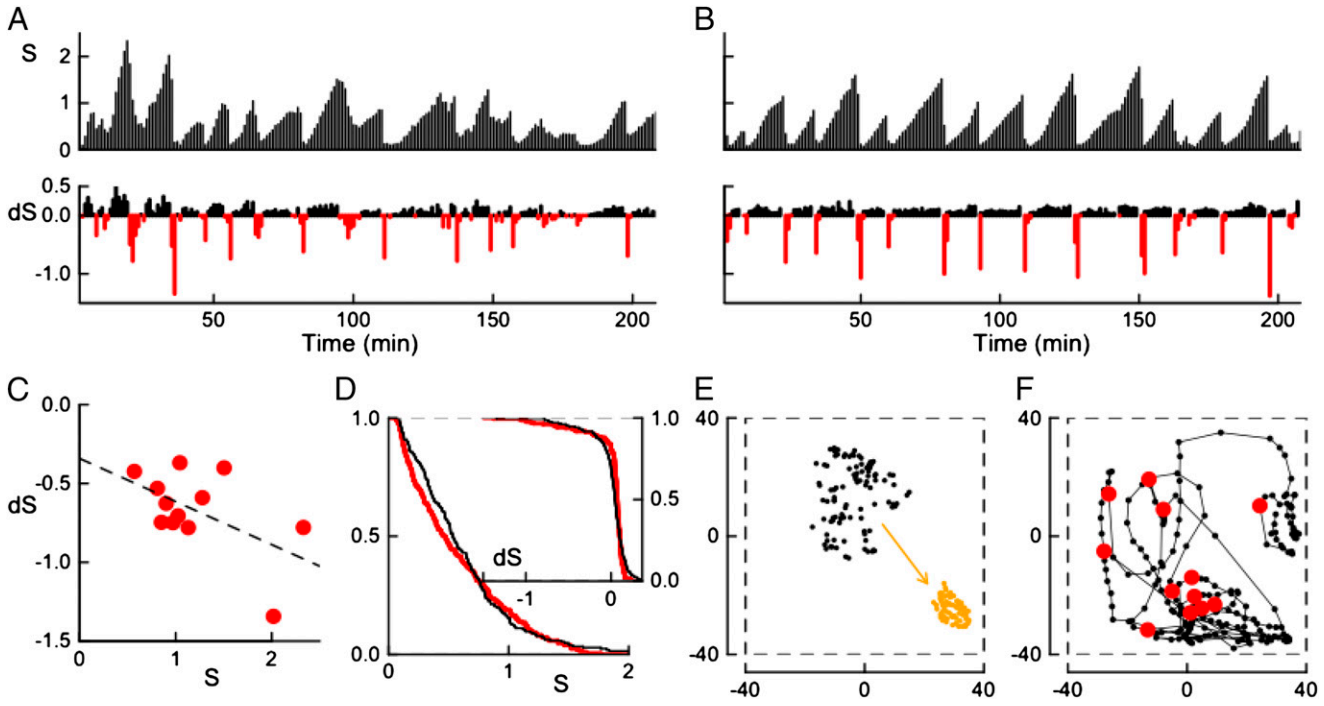

Fig. 1. (*A*) Experimental time series of the group area $S(t)$ (× 1,000 m^2) and its changes over 1 min $dS(t)$ (× 1,000 m^2) as a function of time. $S(t)$ displays the intriguing ratchet-like temporal patterns with slow increases, corresponding to $dS(t)\geq 0$ (in black), abruptly interrupted by fast packing events corresponding to $dS(t)\ll 0$ (in red). (*B*) Same quantities as obtained from a typical simulation of our model (see *Numerical Simulations*). (*C*) Parametric plot of $dS(t)$ vs. $S(t)$ for the major packing events ($dS(t)\leq -0.35\times 1{,}000$ m^2). The dashed line marks linear regression with a linear coefficient equal to −0.27 (with a *P* value of 0.07). (*D*) Empirical CCDF of $S(t)$ (black), compared with the model one extracted from *B* (red). (*Inset*) CCDFs of experimental $dS(t)$ (black) and model prediction (red). (*E*) Two typical experimental snapshots are shown within paddock boundaries (fence, dotted line): a dispersed group (at $t=110$ min, black dots) immediately precedes a packing event, and a compact one (at $t=112$ min, orange dots) follows it. (*F*) Trajectory of the center of mass of the experimental group. The red dots mark the starting position of the major packing events. The observation tower is located outside the fence, near the bottom left corner of *E* and *F*. Error bars for *S*, *dS*, and the center of mass positions due to individual sheep tracking errors are negligible on the shown scales.

yielding an extension ratio of about 30 (i.e., sheep density varied from 1.3 individuals per square meter up to around 1 sheep in 23 m^2). After each packing event, the herd is dense and homogeneous, with an interindividual distance of about 1 m. In the dispersed configurations, on the other hand, sheep are not homogeneously distributed. Typical diluted and dense configurations are shown in Fig. 1*E*. The maximum surface occupied is only about 37% of the arena surface, indicating that packing events are likely not induced by the group saturating the available grazing area. Over time, the group explored the entire arena, and the location of packing events changed, indicating that they are not correlated with a preferred spot on the field or its boundary (see Fig. 1*F*).

Individual sheep velocities allow for further analysis. Not surprisingly, their orientation coincides rather well with the instantaneous headings $\mathbf{s}_i^t$ (Pearson correlation coefficient $c = 0.64$, with a P value smaller then 10^{-6}), the mismatch being due to tracking errors and the discrete-time sampling. The speed of the center of mass (or the group speed), measured by the average speed $v_{cm}^t = \left|\langle \mathbf{v}_i^t \rangle\right|$ (where $\langle \cdot \rangle$ indicates average over the entire group), also shows spiking behavior (see Fig. 2*A*), strongly correlated with the fast contractions of the group area (its correlation coefficient with dS being $c = -0.47$, P value less then $5 \cdot 10^{-6}$; see also *Additional Data Analysis*). Note that, assuming statistical independency of the individual sheep tracking errors, one estimates the total error on group speed to be $\Delta v/\sqrt{100} = 0.03$ m/s. Because large spikes in v_{cm}^t can only be generated by the coordinated run of many sheep, they are a good proxy for the amplitude of packing events. [It is better, for instance, than the macroscopic polarization $\mathbf{P}^t = \langle \mathbf{s}_i^t \rangle_i$ of the herd, which shows smaller correlation with the packing events (see Fig. S2).] The probability distribution of v_{cm} shows packing events on practically all accessible scales (Fig. 2*B*) given a maximum recorded individual speed of about 1.5 m/s. Its functional form is compatible with a shoulder at small speed followed by a power-law tail with exponent $\gamma = -2.3(2)$. Given the limited amount of data and the strong intrinsic noise, one has to cautiously consider this algebraic decay. Indeed, considering instead the complementary cumulative distribution function (CCDF) in lin–log scales reveals the possible superposition of two exponentials (Fig. 2*C*). [The CCDF $F_v(v_{cm}) = P(v > v_{cm})$ gives the probability that the observed variable v takes a value greater than v_{cm}.] On the other hand, in log–log scales, the CCDF still shows a believable algebraic tail (Fig. 2*D*), albeit with an estimated decay exponent $(\gamma + 1) = -1.6(2)$ (see *Discussion*). Finally, for a discussion of the herd center of mass displacement we refer the reader to Fig. S3*A*.

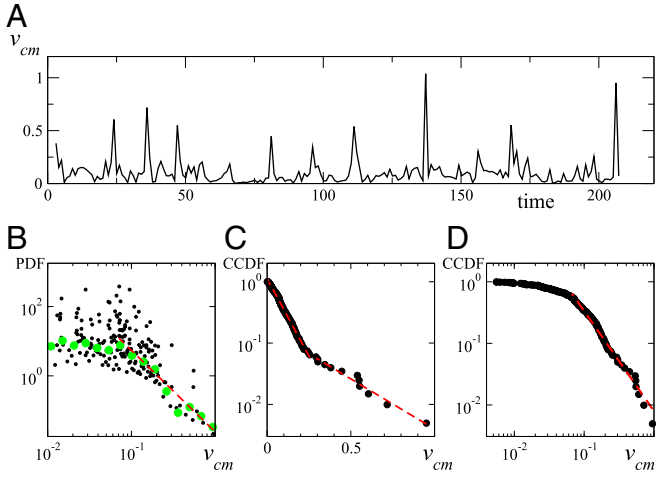

Fig. 2. (*A*) Center of mass speed v_{cm} (meters per second) vs. time (in minutes). (*B*) Log–log plot of the PDF of v_{cm}. Black dots have been obtained by differencing the CCDF obtained by a proper ordering of the data of *A*, and they do not depend on binning procedure or any other data treatment. Green dots represent a logarithmic binning of the same data. Red dashed line is best power-law fit (with $v_{cm} \leq 0.07$) with exponent −2.3(2). (*C*) CCDF in lin–log scale (black dots). Red dashed lines are exponential fits below and above $v_{cm} = 0.23$ with respective characteristic scales ∼0.086 and ∼0.27. (*D*) CCDF in log–log scales (black dots). Red dashed line is best power-law fit for $v_{cm} \geq 0.07$ with exponent −1.6(2).

Spatial Analysis of a Packing Event and Quantification of Individual Behavior. To gain insight on the local, individual mechanisms involved, we analyzed the spatial structure of packing, fast-moving events. We first established a simple quantitative criterion for distinguishing, at each time step, the individuals actively taking part in the packing events from those exhibiting grazing behavior. To this aim, we analyzed the total distribution of individual speeds $v_i = \|\mathbf{v}_i\|$. It clearly comprises three parts, allowing not only the sorting out of the fast-moving individuals but also the distinguishing of walking from stationary sheep: On average, a large majority (74%) of sheep are actually motionless ($v = 0$ at our resolution). The probability distribution $P(v)$ of the speed of moving sheep shows a primary peak at $v \approx 0.1$ m/s and a secondary shoulder around $v \approx 0.66$ m/s (see Fig. S4*A*). It can be fitted nicely by the sum of a Poissonian and a (skewed) Gaussian distribution, corresponding, respectively, to walking and running individuals. We can use the crossing value of these two distributions, at $\tilde{v} \simeq 0.41$ m/s, as a practical threshold to distinguish walking from running individuals. Thus, a given sheep can be found in any of three well-defined behavioral states, stationary, walking, or running, switching frequently between them. An analysis of packing events in terms of the fraction of running individuals bears the same intermittent behavior as the one exhibited by the group center of mass speed, testifying to the consistency of our behavioral classification (see Fig. S4 *B–D*).

We performed a complete second-by-second tracking of one of the largest and fastest packing events. In Fig. 3, we show five configurations extracted from this sequence. (The full 2-min sequence is available as Movie S3.) Sheep are colored according to their speed, corresponding to the stationary, walking, or running state. Just before the beginning of the event ($t \approx 4{,}790$ s), the herd is spread over a large fraction of the arena, with, in particular, a characteristic "exploring front" (near the top on Fig. 3, *Left*). Soon after, a few of the outermost individuals turn back toward the center of the group and start running, quickly but progressively recruiting more and more individuals in the running state, as in some local imitation process ($t = 4{,}794$, $4{,}802$ s). [Note that this is reminiscent of the collective decision-making mechanism exhibited by starling flocks in turning events (32).] At $t = 4{,}818$ s, almost the entire group is running as a dense herd. Sheep then stop rather quickly and synchronously, leaving a compact herd, which then slowly resumes grazing ($t = 4{,}842$ s). The wavelike propagation of recruitment into the running group and the coordinated halt of the herd when it gets closely packed suggest that (*i*) allelomimetic effects based on local interactions play a role in both the initiation and the inhibition of the packing event and (*ii*) running behavior is inhibited when neighbors become close enough. Time series of several dynamical descriptors during the packing event, confirming this observation, can be found in Fig. S5. Visual inspection of the whole raw data indicates that the features uncovered above are not specific to the particular event studied in detail.

Individual-Based Model for Sheep Collective Behavior

To better understand the role of individual interactions in the emergence of the collective dynamics described above, we present a simple agent-based model that faithfully accounts for the observed density oscillations and the intermittency features of sheep collective dynamics.

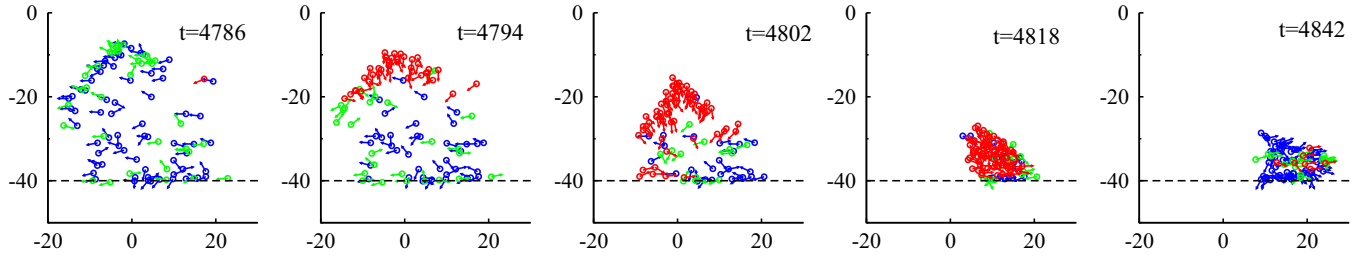

Fig. 3. Details of a single packing event: Five consecutive snapshots are shown, taken at different time steps between $t = 4{,}786$ s and $t = 4{,}842$ s. Colors encode sheep behavior according to their speed v: blue sheep are stationary, green ones are walking ($0 < v \le \bar{v} = 0.41$ m/s), and red are running $v > \bar{v}$. Individual sheep orientations are marked by small arrows. The dashed black line marks the position of the fence. Note that the packing event is initiated by individuals far from the fence.

Current models for the collective motion of animals cannot reproduce the complex avalanche dynamics highlighted by our observations. They assume that social interactions between individuals are local and can be expressed as a combination of alignment (33–35) and attraction/repulsion forces (36–38). If attraction is too weak, groups in open space are not able to maintain cohesion, and they eventually disperse in a diffusive manner. Strong enough attraction/repulsion forces, on the other hand, stabilize group size and typically yield a well-defined mean interindividual distance.

The model we present below is different. Although we do not claim that its rules are the only ones able to reproduce our experimental observations, or even that they faithfully correspond to the biological stimulus/response function of individual Merino sheep, it is useful as a proof of principle; that is, it offers insights on the kind of simple local individual interaction rules from which the sheep collective behavior may emerge. All of the rules encoded in the equations below directly follow from our observations.

Sheep Motion. Sheep are represented by point-like agents able to perceive and respond to their local environment. The state of the ith sheep is given by its position $\mathbf{r}_i^t$, its heading orientation θ_i^t, and its behavioral state $q_i^t \in \{0,1,2\}$, coding, respectively, for stationary, walking, and running. Stationary sheep do not move or change their orientation, but walking and running sheeps' position and heading evolve according to a set of Vicsek-like discrete-time equations,

$$\mathbf{r}_i^{t+\Delta t} = \mathbf{r}_i^t + \Delta t\, v\left(q_i^t\right) \mathbf{s}_i^{t+\Delta t}, \qquad [1]$$

$$\theta_i^{t+\Delta t} = \mathrm{Arg}\left[\sum_{j\in\mathcal{M}_i} \mathbf{s}_j^t\right] + \psi_i^t \quad (\text{if } q_i^t = 1), \qquad [2]$$

$$\theta_i^{t+\Delta t} = \mathrm{Arg}\sum_{j\in\mathcal{V}_i}\left[\delta_{2,q_j^t}\, \mathbf{s}_j^t + \beta\, f\left(r_{ij}^t\right)\mathbf{e}_{ij}^t\right] \quad (\text{if } q_i^t = 2) \qquad [3]$$

where $\mathbf{s}_i^t = (\cos\theta_i^t, \sin\theta_i^t)$ is the heading vector, Δt is the discrete time step, and sheep speed $v(q)$ in Eq. **1** depends on the behavioral state, $v(2) \gg v(1) > v(0) = 0$. Walking sheep ($q = 1$, Eq. **3**) follow a classic Vicsek dynamics: Sheep i tries to align its heading with that of its metric neighbors in $\mathcal{M}_i$, the set of all sheep closer than the interaction distance r_0 against a "noise" term ψ_i^t (a random, delta-correlated angle chosen from a uniform distribution in $[-\eta\pi, \eta\pi]$). (For simplicity, steric repulsion is not implemented explicitly here since the noise avoids individuals to stay "on top of each other.") Eq. **2** leads to the formation of weakly polarized local subgroups of grazing sheep that disperse diffusively in space, creating patterns similar to those observed in the experiments.

Running sheep, on the other hand, follow a more complex heading dynamics, which combines alignment interactions (with other running sheep only) with attraction/repulsion as in ref. 38: In Eq. **3**, $\mathbf{e}_{i,j}^t$ is the unit vector oriented from sheep i to j and $f(r) = \min(1, (r - r_e)/r_e)$ is an attraction/repulsion pairwise force, with equilibrium distance r_e. Because packing events typically occur when sheep are widely spread out, a fixed metric interaction range is not suitable to describe the collective dynamics of running sheep. Recent results in bird flocks (19), fish schools (25), and pedestrians (39) indicate that social vertebrates interact with neighbors chosen according to "topological" (metric-free) rather than metric criteria, such as the closest k neighbors (irrespective of their distance). Here we use the first shell of Voronoi neighbors to define $\mathcal{V}_i$ in Eq. **3**, which then contains almost always the same number of agents, independently of the local density. (See refs. 25 and 40 for details.)

Behavioral States. We finally define the rules for the update of the behavioral state q_i^t, that is, the way sheep change their behavior according to local stimuli. We describe these changes by a set of transition rates between the different behavioral states. Previous experiments conducted on small groups (41, 42) have shown that the probability $p_{0\to1}$ for a stationary individual to start walking is considerably enhanced by the presence of moving neighbors. Here, for the sake of simplicity, we ignore the weaker suppression effect of stationary neighbors and we also assume that $p_{1\to0}$, the inverse transition, possesses the same structure, as suggested in ref. 43. Transitions rates between the stationary and the walking state are thus given as

$$p_{0\to1}(i,t) = \frac{1 + \alpha n_1^t(i)}{\tau_{0\to1}}, \quad p_{1\to0}(i,t) = \frac{1 + \alpha n_0^t(i)}{\tau_{1\to0}}, \qquad [4]$$

where $\tau_{0\to1}$ and $\tau_{0\to1}$ are spontaneous transition times, α measures the strength of mimetic effects, and $n_0^t(i)$, $n_1^t(i)$ is the number of stationary and walking metric neighbors, respectively.

The transitions to and from the running state are similar, but they depend on the number m_R of running topological neighbors, with the allelomimetic effect strengthened by an exponent $\delta > 1$,

$$p_{0,1\to2}(i,t) = \frac{1}{\tau_{0,1\to2}}\left[\frac{\ell_i^t}{d_R}\left(1 + \alpha m_R^t(i)\right)\right]^\delta, \qquad [5]$$

where ℓ_i^t is the mean distance to all topological neighbors of sheep i, and d_R is some characteristic length scale. The ratio between these two scales ensures that spread-out groups are much more likely to trigger a packing event than high-density ones.

Finally, for simplicity, running sheep can only transit to the stationary state with a rate $p_{2\to0}(i,t)$ enhanced by m_S, the number of their stopping topological neighbors, i.e., those that switched from running to stationary in the previous time step,

$$p_{2\to0}(i,t) = \frac{1}{\tau_{2\to0}}\left[\frac{d_S}{\ell_i^t}\left(1 + \alpha m_S^t(i)\right)\right]^\delta, \qquad [6]$$

where $d_S < d_R$ is a second characteristic length. The positive feedback with the stopping neighbors leads to sudden stopping of the

group. Notice that now, here, ℓ_i plays a role opposite to that it had in Eq. **5**: The stopping transition rate is enhanced when the topological neighbors are located at a short distance. We now briefly comment on metric and topological neighbors. Metric neighbors can be associated with the immediate surroundings of the animal and with social interactions characteristic of the grazing phase. Voronoi neighbors, on the other hand, can be thought as the first shell of individuals that can be visually perceived without obstruction from interposing sheep. Our model reflects the fact that sheep are particularly sensitive, in terms of alignment and recruitment into packing runs, to other running individuals that enter their visual range, an event that should trigger some alarm in a species subject to potential predators.

Parameter Estimation and Comparison with Experimental Data. Many model parameters are readily given from experimental data or estimated from orders of magnitude considerations, as detailed in *Agent-Based Model*. In the following, we fix $v_1 = 0.15$ m/s, $v_2 = 1.5$ m/s, $\tau_{1\to0} = 8$ s, $\tau_{0\to1} = 35$ s, $\tau_{0,1\to2} = \tau_{2\to0} = N$ s, $d_S = 6.3$ m, $d_R = 31.6$ m, $r_e = r_0 = 1$ m, $\beta = 0.8$ and $\eta = 0.13$ (see *Supporting Information* for more details). This being done, we are left with two unknowns, the allelomimetic parameters α and δ. Simulations with 100 sheep reveal that dynamics similar to the one observed experimentally, with slow spreading periods followed by much shorter packing events, can be recovered only when there is a high level of imitation, namely when $\alpha > 5$ and $\delta > 2$.

Numerical inspection in the parameter range $\alpha \in [5,25]$ and $\delta \in [2,5]$ reveals that the experimental data are best described with $\alpha \simeq 15$ and $\delta \simeq 4$. Time series of the occupied surface display the same fast packing events and the typical burst pattern of $dS(t)$ (see Fig. 1*B*). The corresponding CCDFs match well the experimental ones (Fig. 1*D*). (Note that the model was simulated in open space, an additional point in favor of the negligible role of the fence in the experiments.) Movie S4 shows a typical run. The model at these optimal parameters also reproduces the intermittency of the center of mass speed v_{cm} (see Fig. S6*A*). Cumulated over a number of events similar to that contained in the experimental data, the probability distribution function (PDF) of v_{cm} shows the same noisy, possibly power-law tail with decay exponent $-2.2(2)$ (Fig. 4*B*), and the CDF is also compatible with the superposition of two exponentials. However, simulated over a very large number of events, power laws are ruled out, whereas the exponential fits become very good (Fig. 4*C*). Pending the discussion of these findings below, a general comment holds: The fact that our model is able to capture the statistical features of density fluctuations as well as the qualitative statistics of the aggregation events, with a single set of parameter values, indicates that our description captures the essential features of the stimulus–response function of individual Merino sheep.

Our main parameters α and δ both control the mean maximum group area S_M reached by the group before a packing event, and the mean time τ_P needed to regroup to a packed configuration. Our simulations (see Fig. 4*A*) show that, for any $\delta > 2$, τ_P yields a minimum as a function of α, with a global minimum located in the parameter range $\delta \in [3,4]$ and $\alpha = [12,17]$. S_M, on the other hand, does not display a global maximum, being a growing function of δ, but our chosen parameter values $\delta = 4$, $\alpha = 15$ seem to represent a good compromise between the competing needs discussed above. We finally note that the two-state grazing dynamics is more important than it may appear at first sight: A simpler dynamics in which all grazing sheep are walking (corresponding to the limit case $\tau_{1\to0} \gg \tau_{0\to1}$) produces far too spatially homogeneous configurations and does not yield a distribution of packing events consistent with the experimental data.

Discussion

We have shown that Merino sheep balance the conflicting needs of social protection and reduced competition when feeding by alternating gentle group-spreading grazing phases with fast packing events that dramatically increase the group density by up to a factor 30. Social cohesion is not reached by settling down to a steady group density but rather is maintained through sudden regroupings. Although such dynamics may be not completely unknown to field biologists, this is, to our knowledge, the first quantitative study of a large group of social herbivores in a well-controlled homogeneous feeding environment. By using homogeneous pastures, we minimize as much as possible the effect of environment heterogeneity (44). Direct predation disturbances that may be invoked to explain increases in group density (12, 13, 45) are also ruled out in this context. Therefore, we are able to argue that this collective behavior mainly results from socially driven individual decisions.

The combination of experimental analyses with the numerical study of a spatially explicit model offers insights on the individual-level stimulus/response functions that can underlie such complex collective phenomena. In particular, our work points to a local origin for packing events: Danger/fear increases with the typical distance to visual/topological neighbors, up to a threshold beyond which running is triggered. A few sheep initiate a wave of recruitment into a running (sub) group, in agreement with earlier observations that vigilance is increased for individuals at the edge of a group (46, 47). Our model shows that local but metric-free interactions, together with strong allelomimetic behavior, are sufficient to generate such complex collective intermittent dynamics. Its main free parameters, α and δ, quantify the gregarious character of our sheep. That they must be chosen with large numerical values to reproduce experimental observations is a measure of the strong allelomimetic behavior of Merino sheep. In this parameter range, spotting a single running individual is often enough to induce a run in other sheep, surely a useful trait in a social animal subjected to predation risks. Moreover, we have shown that these parameter values offer a reasonable compromise between the need to cover a large grazing area and to minimize the time to regroup. Thus, one may conjecture that the ability of sheep

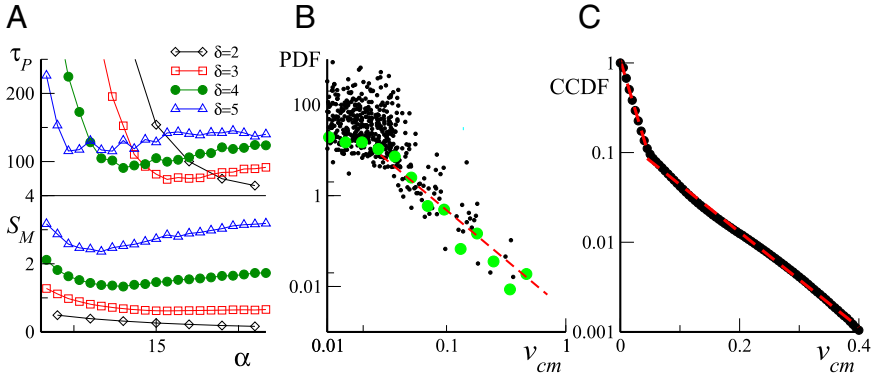

Fig. 4. Model analysis for $N = 100$. (*A*) Packing time τ_P (*Top*) and maximum group area S_M (*Bottom*) as a function of α for different exponents δ. (*B*) PDF of center of mass speed v_{cm} for $\alpha = 15$ and $\delta = 4$ obtained as in Fig. 2. Red dashed line is power-law fit with exponent -2.2. (*C*) Corresponding CCDF in lin–log scales. Red dashed lines are exponential fits with characteristic scales 0.02 and 0.08. Simulations details are given in *Supporting Information*.

to maintain cohesion through such self-organized density oscillations could be linked to a behavioral optimization process within a social context. Such an optimization process could have tuned the strength of allelomimetic interactions between sheep so as to ensure, at the individual scale, a fine balance between (*i*) the need to explore the maximum area of space to avoid interindividual competition when foraging and (*ii*) the need to keep contact with the other group members to ensure cohesion and protection.

Given the elementary nature of the decision-making rules studied here, it is likely that the same phenomenon is present in other social species (48) whenever imperatives for mutual protection and foraging/exploration compete.

We finally discuss the statistics of packing events. Both experiments and model show that they are distributed over all accessible scales. The precise functional form of this distribution remains unclear: A power-law tail remains possible for the field data but is excluded for the model data, which are best accounted for by the superposition of two exponentials. It is thus difficult to decide between two alternatives for the field data: Either they do exhibit power-law behavior (albeit with a decay exponent leading to a well-defined mean event size) and the model is incomplete or they are also best described by the superposition of several exponentials. Further data, especially on larger groups, would thus be highly desirable to shed more light on this point. Note that, to invoke a true self-organized criticality scenario (49), the timescales separation inherent to the behavioral mechanisms described here should likely grow with group size. On the other hand, it has been recently argued that some animal groups, although not truly critical in the rigorous sense, might operate at the maximally critical regime allowed by their (ineluctably) finite size (50).

At any rate, this may be of little biological importance: For all practical purposes, the large sheep herds studied here show the ability to fluctuate and respond fast on a wide range of scales, in line with the general idea that certain biological systems operate in some self-organized, marginally stable regime.

ACKNOWLEDGMENTS. We thank J. Gautrais for field and software assistance and P. M. Bouquet and the staff of the Domaine du Merle for field assistance. This research has been supported by Agence Nationale de la Recherche (ANR) project PANURGE, Project BLAN07-3 200418. F.G. acknowledges support from SUPA, Engineering and Physical Sciences Research Council (EPSRC) First Grant EP/K018450/1 and Marie Curie Career Integration Grant (CIG) PCIG13-GA-2013-618399.

1. Partridge BL, Johansson J, Kalish J (1983) The structure of schools of giant bluefin tuna in Cape Cod Bay. *Environ Biol Fishes* 9(3-4):253–262.
2. Bednarz JC (1988) Cooperative hunting Harris' hawks (*Parabuteo unicinctus*). *Science* 239(4847):1525–1527.
3. Creel S, Creel NM (1995) Communal hunting and pack size in African wild dogs, *Lycaon pictus*. *Anim Behav* 50(5):1325–1339.
4. Handegard NO, et al. (2012) The dynamics of coordinated group hunting and collective information transfer among schooling prey. *Curr Biol* 22(13):1213–1217.
5. Deneubourg JL, Goss S (1989) Collective patterns and decision making. *Ethol Ecol Evol* 1(4):295–311.
6. Seeley TD (2010) *Honeybee Democracy* (Princeton Univ Press, Princeton, NJ).
7. Ballerini M, et al. (2008) Empirical investigation of starling flocks: A benchmark study in collective animal behaviour. *Anim Behav* 76(1):201–215.
8. Foster WA, Treherne JE (1981) Evidence for the dilution effect in the selfish herd from fish predation on a marine insect. *Nature* 293:466–467.
9. Treherne JE, Foster WA (1981) Group transmission of predator avoidance-behavior in a marine insect: The Trafalgar effect. *Anim Behav* 29(3):911–917.
10. Domenici P, Batty RS (1997) Escape behaviour of solitary herring (*Clupea harengus*) and comparisons with schooling individuals. *Mar Biol* 128(1):29–38.
11. Domenici P, Standen EM, Levine RP (2004) Escape manoeuvres in the spiny dogfish (*Squalus acanthias*). *J Exp Biol* 207(Pt 13):2339–2349.
12. Procaccini A, et al. (2011) Propagating waves in starling, *Sturnus vulgaris*, flocks under predation. *Anim Behav* 82(4):759–765.
13. King AJ, et al. (2012) Selfish-herd behaviour of sheep under threat. *Curr Biol* 22(14): R561–R562.
14. Giardina I (2008) Collective behavior in animal groups: Theoretical models and empirical studies. *HFSP J* 2(4):205–219.
15. Vicsek T, Zafeiris A (2012) Collective motion. *Phys Rep* 517(3-4):71–140.
16. Camazine S, et al. (2001) *Self-Organization in Biological Systems* (Princeton Univ Press, Princeton, NJ).
17. Krause J, Ruxton GD (2002) *Living in Groups* (Oxford Univ Press, Oxford).
18. Sumpter DJ (2010) *Collective Animal Behavior* (Princeton Univ Press, Princeton, NJ).
19. Ballerini M, et al. (2008) Interaction ruling animal collective behavior depends on topological rather than metric distance: Evidence from a field study. *Proc Natl Acad Sci USA* 105(4):1232–1237.
20. Buhl J, Sword GA, Simpson SJ (2012) Using field data to test locust migratory band collective movement models. *Interface Focus* 2(6):757–763.
21. Attanasi A, et al. (2014) Collective behaviour without collective order in wild swarms of midges. *PLOS Comput Biol* 10(7):e1003697.
22. Cavagna A, et al. (2010) Scale-free correlations in starling flocks. *Proc Natl Acad Sci USA* 107(26):11865–11870.
23. Katz Y, Tunstrøm K, Ioannou CC, Huepe C, Couzin ID (2011) Inferring the structure and dynamics of interactions in schooling fish. *Proc Natl Acad Sci USA* 108(46):18720–18725.
24. Herbert-Read JE, et al. (2011) Inferring the rules of interaction of shoaling fish. *Proc Natl Acad Sci USA* 108(46):18726–18731.
25. Gautrais J, et al. (2012) Deciphering interactions in moving animal groups. *PLos Comput. Biol* 8(9):e1002678.
26. Puckett JG, Kelley DH, Ouellette NT (2014) Searching for effective forces in laboratory insect swarms. *Sci Rep* 4:4766.
27. Becco C, Vanderwalle N, Delcourt J, Poncin P (2006) Experimental evidences of a structural and dynamical transition in fish school. *Physica A* 367:487–493.
28. Tunstrøm K, et al. (2013) Collective states, multistability and transitional behavior in schooling fish. *PLOS Comput Biol* 9(2):e1002915.
29. Hunter JR (1972) Swimming and feeding behavior of larval anchovy *Engraulis mordax*. *Fish Bull* 70:821–838.
30. Hamner WM (1984) Aspects of schooling in *Euphausia superba*. *J Crustac Biol* 4:67–74.
31. Arnold GW, Dudzinski ML (1978) *The Ethology of Free-Ranging Domestic Animals* (Elsevier, Amsterdam).
32. Attanasi A, et al. (2014) Information transfer and behavioural inertia in starling flocks. *Nat Phys* 10(9):615–698.
33. Vicsek T, Czirók A, Ben-Jacob E, Cohen I, Shochet O (1995) Novel type of phase transition in a system of self-driven particles. *Phys Rev Lett* 75(6):1226–1229.
34. Grégoire G, Chaté H (2004) Onset of collective and cohesive motion. *Phys Rev Lett* 92(2):025702.
35. Chaté H, Ginelli F, Grégoire G, Raynaud F (2008) Collective motion of self-propelled particles interacting without cohesion. *Phys Rev E Stat Nonlin Soft Matter Phys* 77(4 Pt 2):046113.
36. Reynolds C (1987) Flocks, herds and schools: A distributed behavioral model. *Comput Graph* 21(4):25–34.
37. Couzin ID, Krause J, James R, Ruxton GD, Franks NR (2002) Collective memory and spatial sorting in animal groups. *J Theor Biol* 218(1):1–11.
38. Grégoire G, Chaté H, Tu Y (2003) Moving and staying together without a leader. *Phys D* 181(3-4):157–170.
39. Moussaïd M, Helbing D, Theraulaz G (2011) How simple rules determine pedestrian behavior and crowd disasters. *Proc Natl Acad Sci USA* 108(17):6884–6888.
40. Ginelli F, Chaté H (2010) Relevance of metric-free interactions in flocking phenomena. *Phys Rev Lett* 105(16):168103.
41. Pillot MH, et al. (2011) Scalable rules for coherent group motion in a gregarious vertebrate. *PLoS One* 6(1):e14487.
42. Ramseyer A, Boissy A, Dumont B, Thierry B (2009) Decision making in group departures of sheep is a continuous process. *Anim Behav* 78(1):71–78.
43. Gautrais J, et al. (2007) Allelomimetic synchronization in Merino sheep. *Anim Behav* 74(5):1443–1454.
44. Sibbald AM, Oom SP, Hooper RJ, Anderson RM (2008) Effects of social behaviour on the spatial distribution of sheep grazing a complex vegetation mosaic. *Appl Anim Behav Sci* 115(3-4):149–159.
45. Spieler M (2003) Risk of predation affects aggregation size: A study with tadpoles of *Phrynomantis microps* (Anura: Microhylidae). *Anim Behav* 65(1):179–184.
46. Ramseyer A, Petit P, Thierry B (2009) Patterns of group movements in juvenile domestic geese. *J Ethol* 27(3):369–375.
47. Fernandez-Juricic E, Beauchamp G (2008) An experimental analysis of spatial position effects on foraging and vigilance in brown-headed cowbird flocks. *Ethology* 114(2):105–114.
48. Miller NY, Gerlai R (2008) Oscillations in shoal cohesion in zebrafish (*Danio rerio*). *Behav Brain Res* 193(1):148–151.
49. Bak P (1996) *How Nature Works: The Science of Self-Organized Criticality* (Copernicus, New York).
50. Attanasi A, et al. (2014) Finite-size scaling as a way to probe near-criticality in natural swarms. *Phys Rev Lett* 113(23):238102.
51. Mundy JL, Zisserman A, eds (1992) *Geometric Invariance in Computer Vision* (MIT Press, Cambridge, MA).